

Reducing the critical switching current in nanoscale spin valves

Jan Manschot^{1,2}, Arne Brataas², and Gerrit E. W. Bauer¹

*1: Kavli Insitute of Nanoscience, Delft University
of Technology, 2628 CJ Delft, The Netherlands*

*2: Department of Physics, Norwegian University of
Science and Technology, N-7491 Trondheim, Norway*

Abstract

The current induced magnetization reversal in nanoscale spin valves is a potential alternative to magnetic field switching in magnetic memory devices. We show that the critical switching current can be decreased by an order of magnitude by strategically distributing the resistances in the magnetically active region of the spin valve. In addition, we simulate full switching curves and predict a new precessional state.

PACS numbers: 73.63.-b Electronic transport in nanoscale materials and structures -75.47.-m Magneto transport phenomena; materials for magneto transport -75.70.Ak Magnetic properties of monolayers and thin films -85.75.-d Magnetoelectronics; spintronics: devices exploiting spin polarized transport or integrated magnetic fields

The prediction that a spin-polarized current can excite and reverse a magnetization^{1,2} has been amply confirmed by recent experiments.^{3,4,5,6,7} The current-induced magnetization dynamics is interesting as an efficient mechanism to write information into magnetic random access memories as well as to generate microwaves.⁸ Unfortunately, the critical currents for magnetization reversal are still unattractively high.^{9,10} In this Letter, we apply a previously developed microscopic model^{11,12} to understand the critical current in spin valves quantitatively and propose a strategy to reduce it by up to an order of magnitude. We also solve the micromagnetic equations with accurate angle-dependent magnetization torque and spin-pumping¹³ terms and predict switching to a novel precessional state.

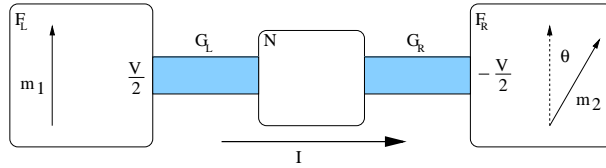


FIG. 1: Schematic picture of a perpendicular spin valve biased by a voltage difference V . θ is the angle between the magnetization directions of both ferromagnetic reservoirs. The reservoirs and contacts need not be identical; the conduction parameters are summarized as G_L and G_R .

Figure 1 presents a generic F(erro)magnetic|N(ormal)|F spin valve with two resistive elements G_L and G_R . Charge and spin currents excited by an applied bias can be calculated accurately with the magneto-electronic circuit theory¹¹ with parameters determined from first-principles band structure calculations¹⁴ that agree well with available experimental data.¹⁵ The resistive elements are characterized by the conductance $g = g^{\uparrow\uparrow} + g^{\downarrow\downarrow}$, the polarization $p = (g^{\uparrow\uparrow} - g^{\downarrow\downarrow})/g$ and the normalized mixing conductance $\eta = 2g^{\uparrow\downarrow}/g$; where $g^{\uparrow\uparrow}$ and $g^{\downarrow\downarrow}$ are, respectively, the conductances for electrons with spin parallel and anti-parallel to the magnetization and $g^{\uparrow\downarrow}$ is the material parameter that governs the magnetization torque. The magnetically active region includes layers of thickness equal to the spin-flip diffusion length from the interfaces. Any resistance outside this region is parasitic and not considered here. The conductances are effective parameters determined by the resistance of the ferromagnetic bulk, that of the interfaces to the normal metal and the resistance of an eventual outer normal metal that fits into the magnetically active region. For simplicity we disregard the bulk resistance of the normal metal island and the imaginary part of $g^{\uparrow\downarrow}$ (for metallic interfaces smaller than 10 % of the real part^{14,16}).

The transverse component of the spin current, *i.e.* the spin torque, is able to excite a magnetization.¹⁶ The torque as function of the angle θ felt by the magnetizations for a symmetrical spin valve is easily calculated by the circuit theory.¹⁵ The analytic expressions for an asymmetrical spin valve are lengthy, however. Numerical results in Ref. 17 proved that the magnetization torque depends strongly on the resistance distribution, even its sign may depend on the asymmetry, as was reported as well by Kovalev *et al.*¹⁸ In order to engineer the asymmetry to our advantage it is very useful to derive analytical results, which is easily achieved for small deviations of the magnetizations from collinearity. In this regime the expression for the magnetization torque can be expanded to lowest order in the non-collinearity. To lowest order in θ the normalized torque $i_s = |\mathbf{m} \times (\mathbf{I}_s \times \mathbf{m})|/I_c$ on the *left* magnetization reads

$$i_s(\theta)|_{\theta \approx 0} = \frac{\hbar}{2e} \left(\frac{g_L \eta_L}{g_L \eta_L + g_R \eta_R} \right) \times \frac{g_R \eta_R (p_R - p_L) + g_L p_R (1 - p_L^2) + g_R p_L (1 - p_R^2)}{g_L (1 - p_L^2) + g_R (1 - p_R^2)} \theta + O(\theta^3). \quad (1)$$

For a symmetrical spin valve ($g_L = g_R$, $p_L = p_R$ and $\eta_L = \eta_R$) we resolve the simple relation $i_s = (\hbar/2e)(p/2)\theta + O(\theta^3)$, that depends only on the polarization and not on the mixing conductance. In an asymmetric structure, $p_R - p_L \neq 0$, the slope of the spin torque can be enhanced considerably.

We investigate a realistic (but non-unique) model for the asymmetry by extending the layer sequence from F|N|F to $N_1|F|N|F|N_2$. We take here the N|F interfaces to be equal and assume that the ferromagnets are thin enough that the bulk contribution is negligibly small. Numerical results require values for the interface resistances that have been measured accurately in the current-perpendicular-to-plane (CPP) geometry.^{19,20} We adopt here Co/Cu interfaces with cross-section $140 \times 90 \text{ nm}^2$, whence $g = 1413 \times 10^3$, $p = 0.75$ and $\eta = 0.38$.^{14,21} The asymmetry is modelled by the normal metal sandwich *outside* the symmetric F|N|F structure. Other asymmetries can be built in and computed with the present method just as well. The conductivity of the resistive element connecting the left (right) reservoir to the adjacent normal metal layer is G_1 (G_2). The asymmetry is expressed by varying the values for G_1 and G_2 for constant series resistance $1/G_1 + 1/G_2 = 0.37 \Omega$, where the latter is a value typical for recently fabricated nanopillars.⁵ We assume the right magnetic layer

is magnetically hard and is treated as static “polarizer”, *e.g.* that it is sufficiently thicker than the free magnetic layer. This does not affect the conductance asymmetry as long as the ferromagnet is highly conductive.

The effective conductance parameters, the conductance \hat{g}_L , polarization \hat{p}_L and relative mixing conductance $\hat{\eta}_L$ for the left hand side of the pillar consisting of the ferromagnet and the outer normal metal can be calculated in terms of the normal metal conductance g_1 as

$$\begin{aligned}\hat{g}_L &= \frac{g_1 g}{2g_1 + g}, \\ \hat{p}_L &= \frac{g_1^2 (g^{\uparrow\uparrow} - g^{\downarrow\downarrow})}{2(g_1 + g^{\uparrow\uparrow})(g_1 + g^{\downarrow\downarrow})g_L}, \\ \hat{\eta}_L &= \frac{2g^{\uparrow\downarrow}}{\hat{g}_L}.\end{aligned}\tag{2}$$

g_1 should be replaced with g_2 to obtain expressions for the right hand side. We parametrize Eq. (1) as $i_s = (\hbar/2e)k\theta + O(\theta^3)$, where numerical results for the torque parameter k are given in Table I for different distributions of the resistance over G_1 and G_2 . We see that for this specific example the spin torque on the left magnetization is enhanced by a factor of five when all normal resistance resides on the side of the *left* magnetic layer. Maximizing the torque on the left magnetization can thus be facilitated by placing a material with a small spin flip length (*e.g.* platinum) adjacent to the *right* magnetic layer and a material with a large spin flip length (*e.g.* copper) to the magnetization layer that has to switch. Note that Pt has been used by Kiselev *et al.*,⁶ but on the side *opposite* to the one recommended by us. The magnitude of the torque is enhanced as well when all resistance is placed on the other side, but it has changed its sign in this case. As shown below, in this configuration an opposite current induces switching to a finite angle.

The magnetization dynamics is described by an extended form of the Landau-Lifshitz-Gilbert equation.^{22,23} As in previous simulations^{24,25} we adopt a macro-spin (single-domain) model, but we take into account improved angle-dependent magnetization torques,¹⁷ as well as the “dynamic stiffness”¹³ due to spin pumping.²⁶ We take the layers to be in the $y - z$ plane and the x -axis in the current direction. The external field, \mathbf{B}_{ext} , and the fixed (right) magnetization are chosen parallel to the z -axis. Temperature induced fluctuations of the magnetizations as well as magnetic anisotropy fields are disregarded for simplicity since they do not interfere with the effect of the distributed resistance.

TABLE I: The slope of the spin torque at $\theta \approx 0$, the increase of the damping by spin pumping and the critical current for different asymmetrical configurations of the investigated finite element system.

$G_1 : G_2$	k	$\Delta\alpha$	$I_{c,c}$
1 : ∞	0.566	0.0054	0.55 mA
1 : 1	0.102	0.0062	3.27 mA
∞ : 1	-0.334	0.0131	-1.57 mA

Analytic estimates of the critical current are possible by focussing on the instability point. When we disregard dipole and exchange coupling between the magnetic layers, both magnetizations in the ground state point along the external field. At the critical current the current-induced torque exactly equals the damping torque $D(\theta)$. The viscous damping reads to lowest order in small deviations in θ from the parallel configuration:

$$D(\theta)|_{\theta \approx 0} = \alpha M_1 B_{\text{ext}} \theta + O(\theta^3), \quad (3)$$

where α is the Gilbert damping parameter, M_1 is the magnitude of the left magnet's magnetic moment and B_{ext} is the magnitude of the external field. We obtain numerical results for M_1 with the sample cross-section defined above, a thickness of 3 nm and a saturation magnetization $M_s = 1.19 \cdot 10^6 \text{ A m}^{-1}$. The critical current $I_{c,c}$ is then simply given by

$$I_{c,c} = \frac{D(\theta)}{i_s(\theta)} \Big|_{\theta \approx 0} = \frac{2e B_{\text{ext}} M_1}{\hbar} \frac{\alpha}{k}. \quad (4)$$

The total Gilbert damping parameter α consists of $\alpha_0 = 0.006$, the bulk Gilbert damping parameter and $\Delta\alpha(\theta)$ originating from the dynamic stiffness,¹³ that depends on the conductance parameters and θ as well.²⁶ We find for $\Delta\alpha(\theta)|_{\theta \approx 0}$ in the limit that the spin currents are efficiently dissipated

$$\Delta\alpha(\theta)|_{\theta \approx 0} = \frac{\gamma \hbar}{8\pi M_1} \left(\frac{2g_1 g^{\uparrow\downarrow}}{g_1 + 2g^{\uparrow\downarrow}} + g^{\uparrow\downarrow} \right). \quad (5)$$

The first term in parentheses is the conductance for a transverse spin current from the (left) ferromagnet to the left reservoir. The transverse spins which escape to the right are

dissipated in the right ferromagnet when $\theta \approx 0$, the conductance for these spins is thus just $\eta g/2$.

The distribution of the resistance over G_1 and G_2 is thus of importance as well for the magnitude of the Gilbert damping. Decreasing g_1 decreases the damping parameter by g_s and thus the critical current. In Table I, the excess damping $\Delta\alpha$ is given for several resistance distributions.

The critical currents $I_{c,c}$ can now be calculated assuming an external field of $B_{\text{ext}} = 0.2$ T. We observe that moving the resistance to the side of the switching layer decreases the critical current in two ways: it both decreases the excess damping and increases the slope of the magnetization torque. For our specific model structure the critical current is six times smaller in the most asymmetric compared to the symmetric pillar. When all resistance resides on the right hand side of the pillar, the lowest critical current is achieved by an opposite bias. Not only the torque, as shown above, but also the damping is then increased. Measured critical currents can be modelled generally well with our model (within 10 %) when anisotropy fields are included and, in some samples, the dynamics of the polarizer. The main inaccuracy is caused by the in general not very well-known (asymmetric) resistance distribution in real spin valves.

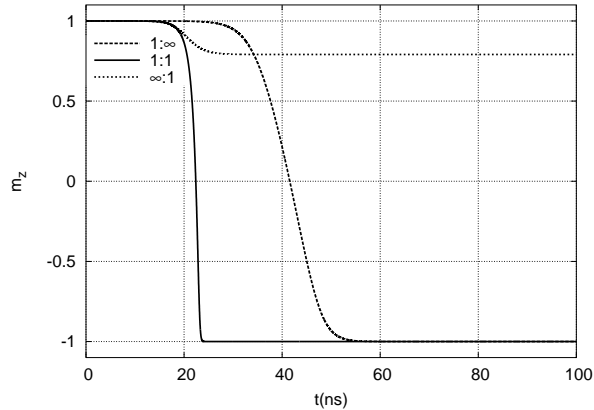


FIG. 2: m_z as function of time for switching in magnetic multilayers with different resistance distributions. The legend denotes the ratio of $G_1 : G_2$.

Finally, we present numerical simulations of complete switching curves. A small initial torque is created by starting at $\theta_0 = 0.001$. In Figure 2 we present the switching curves $m_z(t)$ of the left magnetization for three resistance distributions. $m_z(t)$ is the z -component

of the unit vector $\mathbf{M}_1/|\mathbf{M}_1|$. All curves are calculated with $c = I_c/I_{c,c} = 1.5$. We observe that for $\infty : 1$ the magnetization switches to an angle between 0 and π when the current bias is opposite. The origin of this state clearly differs from previously reported precessional states,^{6,27} which required that the applied field is not parallel to the polarizing (fixed) magnetization. It is a direct consequence of the sign change in the torque as function of the angle.¹⁷

The switching times in the asymmetric samples differ for the same critical current parameter c . One reason for this is the difference in α values. A larger damping parameter increases the critical current but decreases the switching time. The angular dependence of the spin torque affects the switching rate as well; the torque resembles a sine function for the $1 : \infty$ case whereas the symmetrical case is closer to Slonczewski's torque function.¹

Based on analytic expressions for the spin torque and spin pumping near $\theta = 0$ in magnetic multilayers we conclude that the critical current for magnetization reversal in nano-scale spin valves can be reduced by up to an order of magnitude by engineering the resistance distribution in the magnetically active region. The spin torque changes sign for specific asymmetries giving rise to a new precessional state.

This work was financially supported by FOM, the Norwegian Research Council, and the NEDO joint research program "Nano-Scale Magneto-electronics".

-
- ¹ J. C. Slonczewski, J. Magn. Magn. Mater. **159**, L1 (1996).
 - ² L. Berger, Phys. Rev. B **54**, 9353 (1996).
 - ³ R. H. Koch, J. A. Katine, and J. Z. Sun, Phys. Rev. Lett. **92**, 088302 (2004).
 - ⁴ J. A. Katine, F. J. Albert, R. A. Buhrman, E. B. Myers, and D. C. Ralph, Phys. Rev. Lett. **84**, 3149 (2000).
 - ⁵ B. Oezylmaz, A. D. Kent, D. Monsma, J. Z. Sun, M. J. Rooks, and R. H. Koch, Phys. Rev. Lett. **91**, 67203 (2003).
 - ⁶ S. I. Kiselev, J. C. Sankey, I. N. Krivorotov, N. C. Emley, R. J. Schoelkopf, R. A. Buhrman, and D. C. Ralph, Nature **425**, 380 (2003).
 - ⁷ S. Urazhdin, O. Norman, W. P. Pratt Jr., and J. Bass, Phys. Rev. Lett. **91**, 146803 (2003).
 - ⁸ W. H. Rippard, M. R. Pufall, S. Kaka, S. E. Russek, and T. J. Silva, Phys. Rev. Lett. **92** (2004).

- ⁹ J. Z. Sun, *Nature* **425**, 359 (2003).
- ¹⁰ S. Urazhdin, N. O. Birge, W. P. Pratt Jr., and J. Bass (2003), cond-mat/0309191.
- ¹¹ A. Brataas, Y. V. Nazarov, and G. E. W. Bauer, *Phys. Rev. Lett.* **84**, 2481 (2000).
- ¹² A. Brataas, Y. V. Nazarov, and G. E. W. Bauer, *Eur. Phys. J. B* **22**, 99 (2001).
- ¹³ Y. Tserkovnyak, A. Brataas, and G. E. W. Bauer, *Phys. Rev. Lett.* **88**, 117601 (2002).
- ¹⁴ K. Xia, P. J. Kelly, G. E. W. Bauer, A. Brataas, and I. Turek, *Phys. Rev. B* **65**, 220401 (2002).
- ¹⁵ G. E. W. Bauer, Y. Tserkovnyak, D. Huertas-Hernando, and A. Brataas, *Phys. Rev. B* **67**, 94421 (2003).
- ¹⁶ M. D. Stiles and A. Zangwill, *Phys. Rev. B* **66**, 14407 (2002).
- ¹⁷ J. Manschot, A. Brataas, and G. E. W. Bauer, *Phys. Rev. B* **69**, 092407 (2004).
- ¹⁸ A. A. Kovalev, A. Brataas, and G. E. W. Bauer, *Phys. Rev. B* **66**, 224424 (2002).
- ¹⁹ W. P. Pratt Jr., S. F. Lee, J. M. Slaughter, R. Loloee, P. A. Schroeder, and J. Bass, *Phys. Rev. Lett.* **66**, 3060 (1991).
- ²⁰ M. A. M. Gijs, S. K. J. Lenzowski, and J. B. Giesbers, *Phys. Rev. Lett.* **70**, 3343 (1993).
- ²¹ Q. Yang, P. Holody, R. Loloee, L. L. Henry, W. P. Pratt Jr., P. A. Schroeder, and J. Bass, *Phys. Rev. B* **51**, 3226 (1995).
- ²² E. M. Lifshitz and L. P. Pitaevskii, *Statistical Physics, Part 2* (Pergamon Press, 1980).
- ²³ T. L. Gilbert, *Phys. Rev.* **100**, 1243 (1955).
- ²⁴ J. Z. Sun, *Phys. Rev. B* **62** (2000).
- ²⁵ Z. Li and S. Zhang (2003), cond-mat/0302339.
- ²⁶ Y. Tserkovnyak, A. Brataas, and G. E. W. Bauer, *Phys. Rev. B* **67**, 140404 (2003).
- ²⁷ Z. Li and S. Zhang, *Phys. Rev. B* **68**, 024404 (2003).